Electronic supplementary information (ESI)

Composite of Li-Mg-N-H as H_2 storage material: a case study with $Mg(NH_2)_2$-4LiH-$LiNH_2$

Biswajit Paik, [a] *Hai-Wen Li,** [a,b] *Jianhui Wang* [a,c] *and Etsuo Akiba* [a,b,d]

[a] International Research Centre for Hydrogen Energy, Kyushu University, Fukuoka, Japan. E-mail: paik.biswajit.882@m.kyushu-u.ac.jp.
[b] International Institute for Carbon-Neutral Energy Research (WPI-I2CNR), Kyushu University, Fukuoka, Japan. E-mail: li.haiwen.305@m.kyushu-u.ac.jp.
[c] Department of Chemical System Engineering, The University of Tokyo, Tokyo, Japan. E-mail:well.wjh@gmail.com.
[d] Faculty of Engineering, Mechanical Engineering, Kyushu University, Fukuoka, Japan. E-mail:e.akiba@mech.kyushu-u.ac.jp.

A. Reversibility of the dehydrogenation reactions

The reversibility of the hydrogen sorption reaction requires the starting phases to be fully recoverable after re-hydrogenation. To verify the reversibility of the hydrogen sorption in the $Mg(NH_2)_2$-4LiH-$LiNH_2$ composite, we collect the XRD pattern of the powder composite after the 1st hydrogenation cycle carried out in the PCT. The XRD pattern is already shown in Fig. 3 in the main text and the three starting compounds, viz., Mg-amide, LiH and Li-amide have been identified in the re-hydrogenated sample.

A complimentary study to confirm the reversibility of the chemical reactions and the phases has been carried out by the Raman spectroscopy. The Raman view of the phase reversal has been shown in Fig. S1 below by tracking the N-H vibration. Fig. S1 shows the change in the N-H vibration when the ball-milled $Mg(NH_2)_2$-4LiH-$LiNH_2$ is dehydrogenated at 500 ^{0}C (by TG) and is re-hydrogenated again at 160 ^{0}C in the PCT. Fig. S1 also includes Raman spectra of the as-received $Mg(NH_2)_2$ and $LiNH_2$ to compare the vibrational peaks in the composites with those observed in the as-received amides. The as-received amides show vibrational peaks which are close to the reported values. The observed Raman peaks in $LiNH_2$ are 3256 cm^{-1} and 3316 cm^{-1} which may be assigned to the symmetrical and asymmetrical vibrations of NH_2 at wavenumbers 3258 cm^{-1} and 3318 cm^{-1}, respectively [1]. On the other hand, the observed peaks for the

$Mg(NH_2)_2$ are 3268 cm^{-1} and 3320 cm^{-1} which may be assigned to the NH and NH_2 vibrations at 3277 cm^{-1} and 3326 cm^{-1},respectively [2]. Comparing the peaks of 3248 cm^{-1} and 3304 cm^{-1} observed in the as-milled $Mg(NH_2)_2$-4LiH-$LiNH_2$ composite, with those observed in the as-received amides, it may be concluded that the NH_x vibrations in the composite are largely unaffected by the ball-milling and, presumably, no new phase including the imides (shows vibrational peaks, typically, below 3200 cm^{-1}) has been formed during milling. A marginal red shift of the Raman peaks (3248 cm^{-1}) in the ball-milled composite, in comparison to the as-received amides, are probably due to the destabilization of the NH_x bonds by the milling. The dehydrogenated composite at 500 °C contains a broad peak around 3170 cm^{-1}. As we notice from the XRD profile of this sample (Fig. 3, pattern (C) in the main text), the only possible NH vibration may come from the stoichiometric and non-stoichiometric Li_2NH phases. Therefore, we assign the peak at 3170 cm^{-1} to be from these imide phases. This peak disappears upon hydrogen uptake and the characteristics peaks corresponding to the $Mg(NH_2)_2$ and $LiNH_2$ re-appear, albeit, with marginal overlapping due to close proximity of the peak positions.

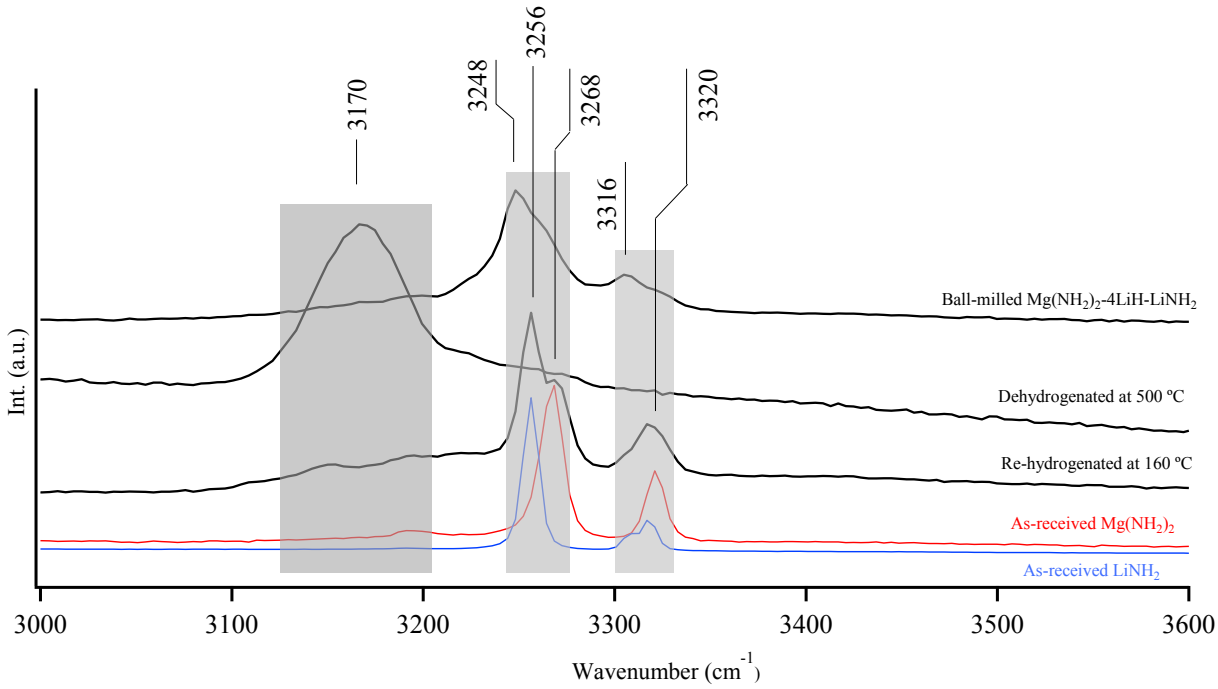

Fig. S1: Raman spectra of the $Mg(NH_2)_2$-4LiH-$LiNH_2$ composite after ball-milling, after dehydrogenation at 500 °C (TG) and re-hydrogenation at 160 °C (PCT). As-received $Mg(NH_2)_2$ and $LiNH_2$ are given as references.

B. Kinetics of the reactions

The isothermal mass-loss profiles provides the information about the nature of the solid-state reactions responsible for the hydrogen desorption and the consequent mass-loss. Several models (1-D, 2-D and 3-D) of diffusion controlled, nucleation controlled and phase-boundary controlled reactions are considered for the present composite to estimate the value of $f(\alpha)$ where α is the fraction of reacted mass related with time t through the relation $f(\alpha)=k.t$; k being the rate constant and depends on the model. These estimated $f(\alpha)$ values are then compared with the calculated $f(\alpha)$ as suggested by Sharp *et al* [3]. Experimental data of temporal isothermal mass-loss at three temperatures 140, 155 and 180 °C are shown in Fig. S2. The $f(\alpha)$ are extracted from these profiles and the values are compared with calculated $f(\alpha)$ values taken from ref [3] in Table S1 showing the typical $f(\alpha)$ estimated from the data obtained at 140 °C and 180 °C. The comparison reveals that the early part of the mass-loss (up to ~4.5 wt%) comes due to the phase-boundary

and nucleation controlled solid-state reactions. However, at the advanced stage of the decomposition (for example, $\alpha > 0.5$ for the isothermal mass-loss at 180 °C), the dehydrogenation is mainly controlled by the diffusion. Phase boundary controlled and diffusion controlled reactions have been identified in several reports to be the probable rate limiting steps for the Li-Mg-N-H systems [4, 5].

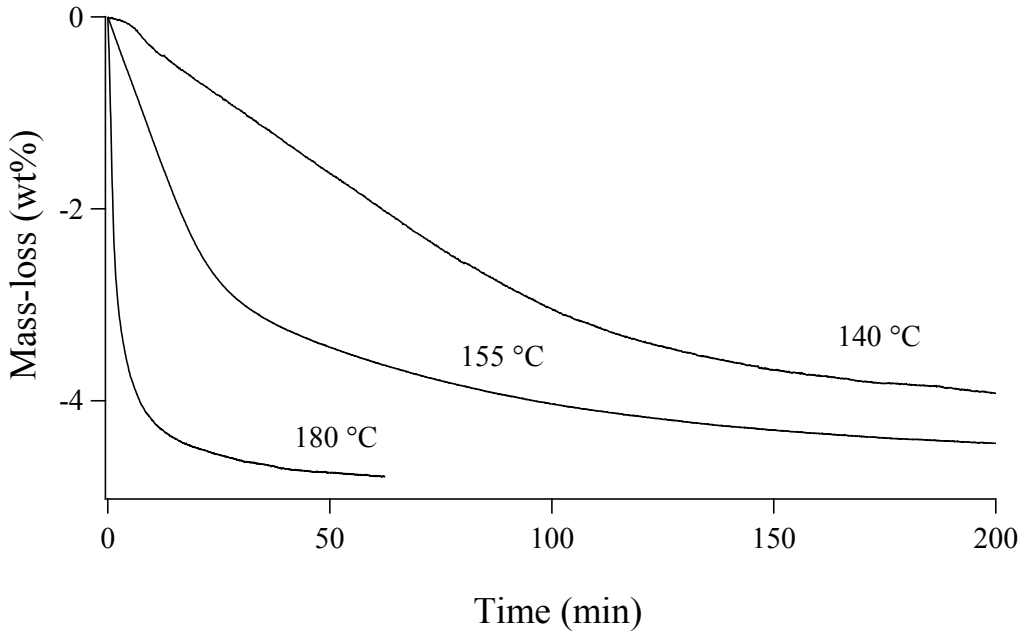

Fig. S2: Isothermal mass-loss profiles of the as-milled composite at 140, 155 and 180 ^{0}C. The reaction models are identified by analyzing these profiles (see Table S1).

Table S1: Comparison between calculated and estimated f(α)=k.t where α is fraction of material reacted in time t, k is the rate constant depending on reaction models (D for diffusion controlled, R for phase boundary-controlled, A for nucleation controlled reactions; 1, 2, 3 indicates 1-D, 2-D and 3-D; F1 is for 1st order reaction. For details of the models and the method to estimate f(α) experimentally, see ref [3].

	Calculated values of f(α)									Exp f(α)	
α	D1	D2	D3	D4	F1	R2	R3	A2	A3	@140 ºC	@180 ºC
0.1	0.040	0.033	0.028	0.032	0.152	0.174	0.165	0.390	0.533	0.20	0.24
0.2	0.160	0.140	0.121	0.135	0.322	0.362	0.349	0.567	0.685	0.38	0.44
0.3	0.360	0.328	0.295	0.324	0.515	0.556	0.544	0.717	0.801	0.58	0.59
0.4	0.640	0.609	0.576	0.595	0.737	0.768	0.762	0.858	0.903	0.78	0.79
0.5	1.0	1.0	1.0	1.0	1.0	1.0	1.0	1.0	1.0	1.0	1.0
0.6	1.440	1.521	1.628	1.541	1.322	1.253	1.277	1.150	1.097	1.22	1.45
0.7	1.960	2.207	2.568	2.297	1.737	1.543	1.607	1.318	1.198	1.51	2.31
0.8	2.560	3.115	4.051	3.378	2.322	1.887	2.014	1.524	1.322	1.96	4.0
0.9	3.240	4.363	6.747	5.028	3.322	2.334	2.602	1.822	1.492	3.28	8.65

Following these reports, we also attempt to quantify the kinetic barrier by estimating the activation energy (E_a) of the dehydrogenation using the Kissinger method using the DSC data obtained from $Mg(NH_2)_2$-4LiH-$LiNH_2$ composite (Fig. S3). The estimated activation energy (E_a) is 133.85 kL/mole. This value is rather high when compared with the E_a estimated for the $Mg(NH_2)_2$-2LiH system (~ 88 kL/mole) [5]. In fact, the E_a of $Mg(NH_2)_2$-4LiH-$LiNH_2$ is not less than that (E_a~130 kL/mole) of the decomposition of $Mg(NH_2)_2$ to release NH_3 [5]. However, the high E_a for the $Mg(NH_2)_2$-4LiH-$LiNH_2$ composite is not related to ammonia release, as is discussed below, and may be a combined effect of rate limiting steps in the phase-boundary controlled reactions as well as diffusion controlled reactions which are dominating, respectively, the early and advance stage of the dehydrogenation. Further investigation is required to clarifying this issue.

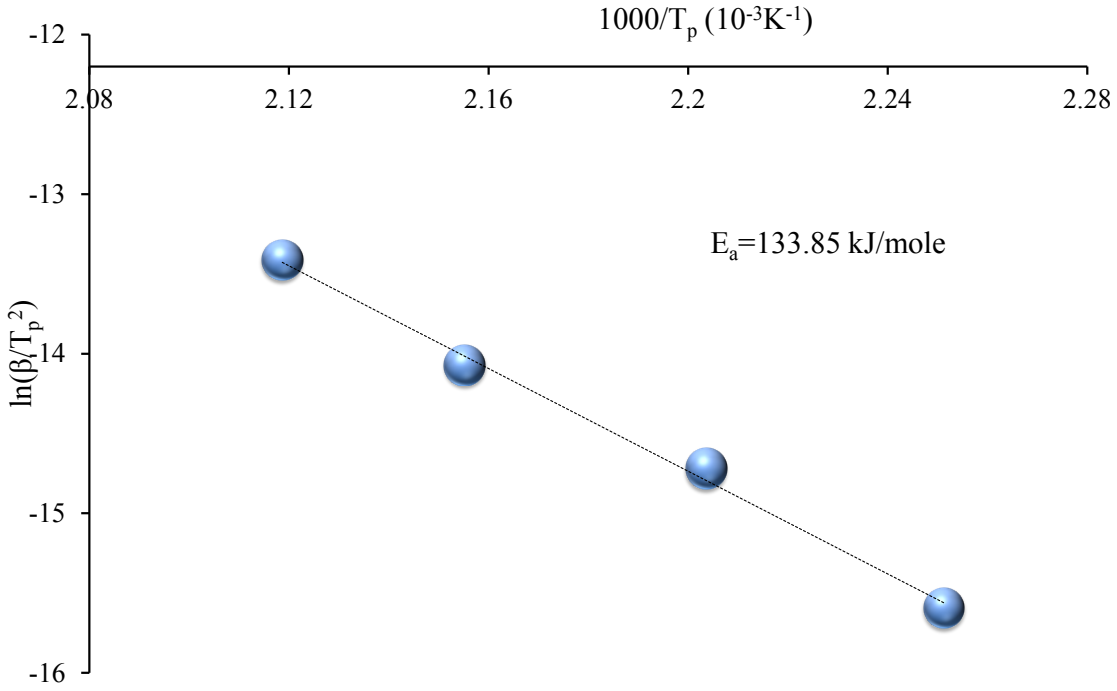

Fig. S3: Kissinger plot for $Mg(NH_2)_2$-4LiH-$LiNH_2$ composite using the temperature (T_p, in kelvin) of the DSC peak (endothermic) and the corresponding heating rate (β, in kelvin/sec) obtained at four different heating rates (2, 5, 10, 20 °/min) under ~ 0.1 MPa He pressure. The estimated activation energy (E_a) is 134 kJ/mole and frequency factor (A) is 15.47×10^{12}/sec according to the Kissinger relation $ln\left(\frac{\beta}{T_p^2}\right) = ln\left(\frac{A.R}{E_a}\right) - \frac{E_a}{R}\left(\frac{1}{T_p}\right)$; R is gas constant.

References

1 J. P. O. Bohger, R. R. Eßmann, H. Jacobs, *J. Mol. Struct*., 1995, **348**, 325.

2 V. G. Linde, R. Juza, *Z. Anorg. Allg. Chem*., 1974, **409**, 199.

3 J. H. Sharp, G.W. Brindley, B.N. Narahari Achar, *J. Amer. Ceram. Soc.*, 1966, **49**, 379.

4 Y. Liu, K. Zhong, K. Luo, M. Gao, H. Pan, Q. Wang, *J. Amer. Chem. Soc.*, 2009, **131**, 1862.

5 P. Chen, Z. Xiong, L. Yang, G. Wu, W. Luo, *J. Phys. Chem. B*, 2006, **110**, 14221.